

# Interpretation of high poling effects with short lifetimes

Carl J. Marckmann

*NKT Research & Innovation A/S, Diplomvej, DTU Bygning 373, DK-2800 Kgs. Lyngby, Denmark*  
*cjm@com.dtu.dk*

Rune Shim, Yitao Ren, and Martin Kristensen  
*COM, DTU Bygning 345v, DK-2800 Kgs. Lyngby, Denmark*  
*rune@com.dtu.dk, yr@com.dtu.dk, and mk@com.dtu.dk*

This paper gives a possible interpretation of the high valued, short lived, linear electro-optic coefficients obtained by some groups. The effect may partly be explained by cracks in the waveguide/fiber system reducing the effective electrode-distance.

**Keywords:** Amorphous materials, electro-optic devices, electro-optic Kerr effect, electro-optic measurements, Pockels effect, poling

## Introduction

Induction of a linear electro-optic effect in silica glass was first obtained in 1991 by Myers *et al* [1] through thermal poling. This discovery opened a door to glass based switches, modulators and tunable filters etc. Unfortunately, the thermal poling induced effect is still too small or decays too fast [2] to be used for industrial purposes.

## Sample preparation

The two samples described in this article consist of a buffer layer made by thermal oxidation of Sb doped Si ( $\sim 3.3\mu m$ ), an etched core ( $\sim 2.0\mu m$  high and  $\sim 4.0\mu m$  wide) and either a hard top-cladding,  $SiO_2$  (sample 3\_5\_1), or a soft top-cladding,  $B, P : SiO_2$  (sample 17\_1). The core and the top-cladding layers were deposited using Plasma Enhanced Chemical Vapour Deposition. The total height of the glass-layers is  $9.5\mu m$  for sample 17\_1 and  $14.5\mu m$  for sample 3\_5\_1. The core was doped with germanium in order to make it sensitive to UV light [3] and with nitrogen in order to stabilize the poling due to increased charge trapping density [4] and to be able to make smaller components due to the higher refractive index-step. A Bragg grating was UV-written in the samples using the phase-mask method [5]. Annealing the samples at  $375^\circ C$  for 1.5h ensured that changes measured in the Bragg wavelength in the poling experiments are due to nonlinearities and not annealing effects. Finally, a top-electrode was made covering the region with Bragg gratings and the Si-wafer was used as back-electrode.

## Measurements

Two different types of measurements were performed on the samples. Interferometric measurements [6] were performed to find the induced linear electro-optic coefficient,  $r$ , and the Bragg gratings were used to probe the third-order nonlinearities,  $\chi^{(3)}$ , and the built-in internal electric field,  $E_{int}$ .

## Bragg gratings as probes

The setup for Bragg gratings used as probes is illustrated in Fig. 1. Light from a tunable laser is sent through a polarization controller, then through the sample and into an optical spectrum analyzer. Transmission spectra were recorded with different voltages applied across the samples. Since silica glass is a centrosymmetric material, the change in refractive index  $\Delta n$  as function of electric field  $E$  can be written as

$$\Delta n(E) = \frac{3\chi^{(3)}}{2n} E^2, \quad (1)$$

where  $n$  is the refractive index and  $\chi^{(3)}$  is the third-order nonlinearity. Terms of higher order than  $E^2$  have been neglected. In the charge separation model [7], mobile charges in the glass move towards the electrodes during poling. These charges will predominantly be trapped at the interfaces between core and cladding layers, giving a sheet of charge on each side of the core layer with different polarity, yielding an internal field  $E_{int}$  across the core layer. If an external field is applied, the total field across the sample becomes  $E = E_{int} + E_{ext}$ . Substituting into equation 1 yields [10]

$$E_{int} = \frac{B}{2C}, \quad \chi_{eff}^{(2)} = \frac{nB}{A} \quad \text{and} \quad \chi^{(3)} = \frac{2nC}{3A}, \quad (2)$$

where  $A$ ,  $B$  and  $C$  are coefficients of the parabola  $\lambda_{Bragg}(E) = A + BE_{ext} + CE_{ext}^2$  representing the change in Bragg wavelength as function of the externally applied electric field. <sup>1)</sup>

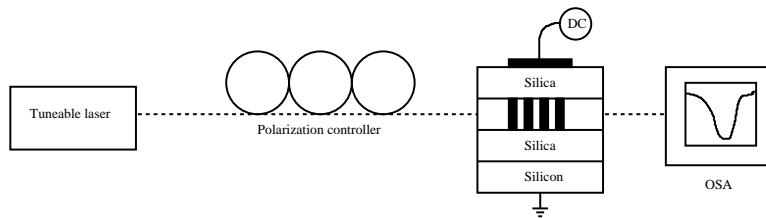


Fig. 1. The setup using Bragg gratings as probes.

## Discussion

From Fig. 2 it is clear that cracks are present in the sample with hard top-cladding, sample 3\_5\_1, but not in the sample with soft top-cladding, sample 17\_1 as in Fig. 3. The breakdown voltage for glass and air is 850 [8] and 3 [9]  $V/\mu m$ , respectively. As the electric fields used in the Bragg grating measurements and used for the thermal poling are stronger than 16  $V/\mu m$  the air-holes/cracks will act as short circuits. Thus, the effective electrode distance in a sample with cracks is much less than the physical electrode separation.

Sample 3\_5\_1 is poled at temperatures as low as room temperature. This is seen in Fig. 4, where the Bragg wavelength is measured in two different sweeps before thermal poling: Firstly, the voltage is swept from 0 to -1.5kV and secondly from -1.5kV to 0.5kV. The step-length in both curves is 0.25kV. The curves are not identical since a field of approximately  $(21.4 \pm 3.3)V/\mu m$  has been built into the sample during the first sweep from 0 to -1.5kV.

Thermal poling of sample 3\_5\_1 at 357°C for 20 minutes at -2.5kV yields a linear electro-optic coefficient between 0.02 and 0.05  $pm/V$  measured right after poling using the interferometric setup. One day after poling,  $r$  has decreased with between 60% and 80% of the initially induced value and one week after poling,  $r$  was measured to zero within the measurement error. The built-in field is thus quasi stable with a lifetime longer than the sweeping time used in the Bragg gratings measurements.

Room temperature poling is not observed in sample 17\_1 as seen in Fig. 5. The two curves are identical within the experimental error and no internal field has been built in during the sweep from 0 to -2.5kV.

<sup>1)</sup>  $r = \frac{2\chi_{eff}^{(2)}}{n^4}$ .

<sup>2)</sup> Under the assumption that there are no cracks i.e. that the effective distance between the electrodes is 14.5  $\mu m$ .

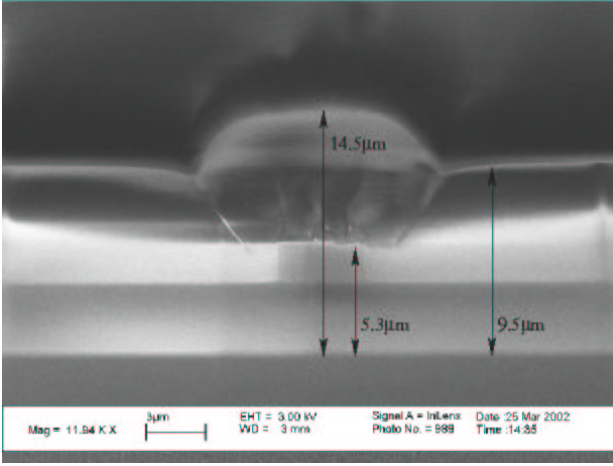


Fig. 2. SEM picture of sample 3\_5\_1. Cracks are clearly visible.

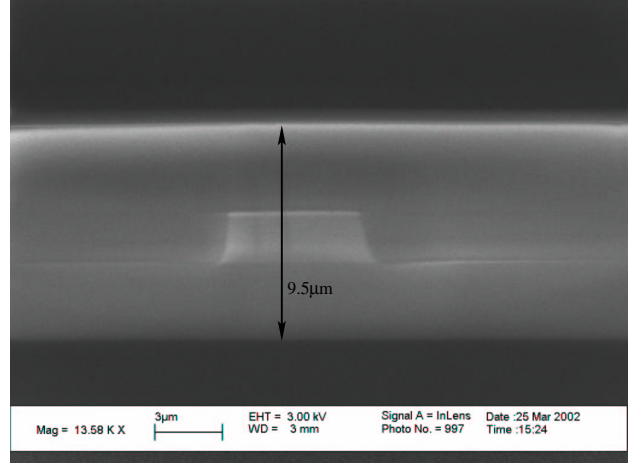


Fig. 3. SEM picture of a  $6\mu m$  wide sample similar to sample 17\_1. No cracks are observed.

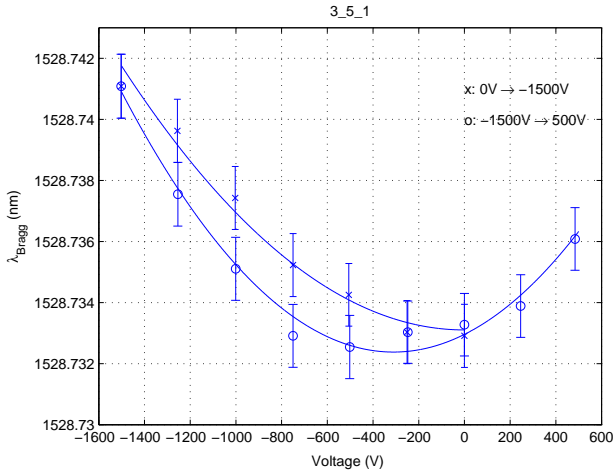


Fig. 4. Sample 3\_5\_1, TE polarization, measured from 0 to -1.5kV and from -1.5 to 0.5kV using the Bragg grating as probe before thermal poling.

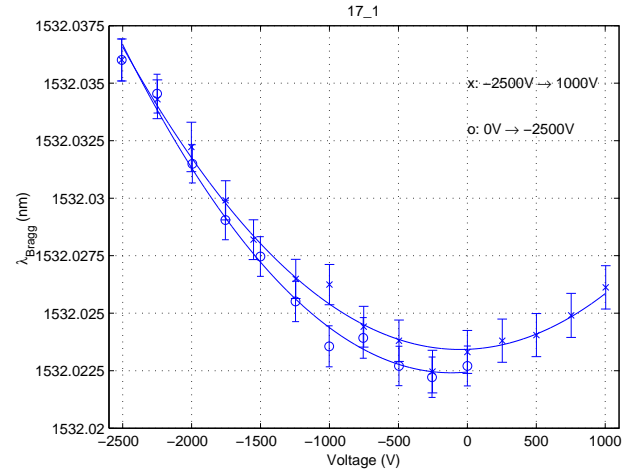


Fig. 5. Sample 17\_1, TE polarization, measured from 0 to -2.5kV and from -2.5 to 1.0kV using the Bragg grating as probe before thermal poling.

From the SEM pictures it is not possible to determine the length of the cracks in sample 3\_5\_1 and therefore the  $\chi^{(3)}$  and induced internal electric field  $E_{int}$  values are calculated for four different effective electrode distances and the values for sample 17\_1 are given for comparison in Table 1. The measurements were performed using the Bragg grating method. The effective electrode distance of  $8.0\mu m$  has been included in Table 1 since it yields the same  $\chi^{(3)}$  value as the one obtained in a previous measurement [10] on a sample with the same core glass as sample 3\_5\_1 but without cracks in the top-cladding.

The instability of the poling induced internal field can also be a result of the cracks, since charges trapped at the interfaces can escape through the cracks. The lifetime of the poling at  $357^\circ C$  might very well exceed the lifetime of the room temperature poling since the charges can be trapped temporarily at the ends of the cracks.

	3_5_1(14.5 $\mu m$ )	3_5_1(9.5 $\mu m$ )	3_5_1(8.0 $\mu m$ )	3_5_1(5.3 $\mu m$ )	17_1
$\chi^{(3)}(10^{-22} \frac{m^2}{V^2})$	$6.46 \pm 0.17$	$2.77 \pm 0.07$	$1.97 \pm 0.05$	$0.86 \pm 0.02$	$1.87 \pm 0.09$
$E_{int}(\frac{V}{\mu m})$	$44.0 \pm 1.7$	$67.2 \pm 2.6$	$79.8 \pm 3.1$	$120.4 \pm 4.6$	$9.8 \pm 3.9$

Table1. The measured values of  $\chi^{(3)}$  and  $E_{int}$  for samples 3\_5\_1 (different effective electrode distances) and 17\_1.

## Conclusion

In this paper we have observed cracks in the hard top-cladding of a sample. Apparently, the measured  $\chi^{(3)} = (6.46 \pm 0.17) \cdot 10^{-22} \frac{m^2}{V^2}$  value of this sample was very high compared to a similar sample [10] without cracks in the top-cladding. The poling-induced  $r$  value had a very short lifetime, in the order of days. This decay time is comparable to the fast decaying  $r$  component seen by others [2]. Both the apparently large  $\chi^{(3)}$  and the fast-decaying  $r$  can be explained by the cracks in the top-cladding since these reduce the effective electrode distance by acting as short-circuits. The apparently large  $\chi^{(3)}$  is caused by the wrong electrode distance used in the calculation of the electric field  $E$ . The fast-decaying  $r$  value can be explained by trapped charges escaping through the cracks. This also explains the room temperature poling as charges can be trapped temporarily at the ends of the cracks when high voltage is applied during measurements. Under the assumption of cracks all the way from the electrodes to the core in [2], the naive corrected  $r$  value is reduced from 0.4 to 0.15 pm/V.

- [1] R. A. Myers, N. Mukherjee and S. R. J. Brueck, "Large second-order nonlinearity in poled fused silica", *Opt. Lett.*, vol. 16, no. 22, pp. 1732-1734, 1991.
- [2] M. Janos, W. Xu, D. Wong, H. Inglis, and S. Fleming, "Growth and Decay of the Electrooptic Effect in Thermally Poled B/Ge Codoped Fiber", *Jour. of Lightwave Tech.*, vol. 17, no. 6, pp. 1037-1041, 1999
- [3] K. O. Hill, Y. Fujii, D. C. Johnson and B. S. Kawasaki, "Photosensitivity in optical fiber waveguides: Application to reflection filter fabrication", *Appl. Phys. Lett.*, vol. 32, no. 10, pp. 647-649, 1978.
- [4] D. Frohman-Bentchkowsky and M. Lenzlinger, "Charge Transport and Storage in Metal-Nitride-Oxide-Silicon (MNOS) Structures", *J. Appl. Phys.*, vol. 40, no. 8, pp. 3307-3319, 1969.
- [5] K. O. Hill, B. Malo, F. Bilodeau, D. C. Johnson and J. Albert, "Bragg gratings fabricated in monomode photosensitive optical fiber by UV exposure through a phase mask", *Appl. Phys. Lett.*, vol 62, no. 10, pp. 1035-1037, 1993.
- [6] Y. Ren, C. J. Marckmann, J. Arentoft, and M. Kristensen, "Thermally poled channel waveguides with polarization independent electro-optic effect", *IEEE Photon. Technol. Lett.*, vol. 14, no. 5, pp. 639-641, May 2002.
- [7] P. G. Kazansky and P. St. J. Russel, "Thermally poled glass: Frozen-in electric field or oriented dipoles?", *Opt. Commun.*, vol. 110, pp. 611-614, 1994.
- [8] F. Haberl, J. Hochreiter, J. Zehetner, and A. J. Schmidt, "Electrical breakdown in ge-doped silica glass fibres", *Int. Jour. of optoelectron.*, vol. 5, no. 4, pp. 363-366, 1990.
- [9] D. K. Cheng, "Fundamentals of engineering electromagnetics", *Addison-Wesley*, pp. 108, 1993.
- [10] C. J. Marckmann, Y. Ren, G. Genty, and M. Kristensen, "Strength and symmetry of the third-order nonlinearity during poling of glass waveguides", *IEEE Photon. Technol. Lett.*, vol. 14, no. 9, pp. 1294-1296, 2002.